


The postcranial anatomy of the saurolophine hadrosaurid *Laiyangosaurus youngi* from the upper cretaceous of Laiyang, Shandong, China

Jialiang Zhang^{1,2}  | Xiaolin Wang^{2,3} | Shunxing Jiang² | Guobiao Li¹

¹School of the Earth Sciences and Resources, China University of Geosciences (Beijing), Beijing, China

²Key Laboratory of Vertebrate Evolution and Human Origins of Chinese Academy of Sciences, Institute of Vertebrate Paleontology and Paleoanthropology, Chinese Academy of Sciences, Beijing, China

³College of Earth and Planetary Sciences, University of Chinese Academy of Sciences, Beijing, China

Correspondence

Xiaolin Wang, Key Laboratory of Vertebrate Evolution and Human Origins of Chinese Academy of Sciences, Institute of Vertebrate Paleontology and Paleoanthropology, Chinese Academy of Sciences, 142 Xizhimenwai Str., Beijing, China.

Email: wangxiaolin@ivpp.ac.cn

Funding information

Laiyang Cretaceous Fauna Research Program of the China University of Geosciences, Beijing, Grant/Award Number: H02657; Laiyang Government Cooperation Dinosaur Project; National Natural Science Foundation of China, Grant/Award Numbers: 41172018, 42288201; Youth Innovation Promotion Association of the Chinese Academy of Sciences, Grant/Award Number: 2019075

Abstract

Laiyangosaurus youngi was erected as a saurolophine hadrosaurid on the basis of several cranial elements from the Jingangkou Formation, Wangshi Group, Upper Cretaceous of Laiyang, Shandong, China. The postcranial elements of this taxon are described in detail here, providing additional postcranial characteristics to *L. youngi*. The phylogenetic analysis included postcranial elements of *L. youngi*, indicating that *L. youngi* still lies in the Edmontosaurini clade and no more supplement of postcranial autapomorphy. However, three new postcranial autapomorphies can help distinguish *L. youngi* from other members of Edmontosaurini: a poorly expanded deltopectoral crest of the humerus, a brevis shelf at the base of the postacetabular process of the ilium, and a well-defined medioventral ridge on the medial side of the postacetabular process. This study is to increase our knowledge on the anatomy and phylogeny of hadrosaurids of Edmontosaurini and provide new valuable evidence for discussing on the taxonomic position and validity of hadrosauroids in the Laiyang Hadrosauroid Fauna.

KEYWORDS

Laiyang, *Laiyangosaurus youngi*, postcranial anatomy, Saurolophinae, Wangshi group

1 | INTRODUCTION

Hadrosauroids were diverse and abundant large herbivorous dinosaurs that lived during the Late Cretaceous (Horner et al., 2004; Prieto-Márquez, 2010a; Wang, You, et al., 2013; Xing, Wang, et al., 2014; You et al., 2003). This lineage of dinosaurs includes some early-diverging forms, also known as non-hadrosaurid hadrosauroids, and the monophyletic Hadrosauridae, which can be divided into two main clades, the Saurolophinae and the

Lambeosaurinae (Prieto-Márquez, 2010b; Wang, You, et al., 2013; Xing, Zhao, et al., 2014). Hadrosauroids were widespread in their distribution between the Aptian and late Maastrichtian, and fossil remains of hadrosauroids have been found in Asia, Europe, North and South America, Africa, and Antarctica (Lund & Gates, 2006; Mateus et al., 2012; Prieto-Márquez, 2010a; Xing, Wang, et al., 2014). A number of fossil hadrosauroids have also been found from the Cretaceous deposits of northern, northeastern, and eastern China (Lund & Gates, 2006;

Wang, You, et al., 2013; Xing, Wang, et al., 2014), particularly from the Upper Cretaceous Wangshi Group of the Laiyang Basin in eastern Shandong Province, China (Figure 1) (Wang et al., 2010, 2012).

The terrestrial Cretaceous strata are well-developed in this basin, consisting of the Lower Cretaceous Laiyang and Qingshan groups and the Upper Cretaceous Wangshi Group (Wang et al., 2010, 2012). The Wangshi Group mainly comprises fluvial and lacustrine red and gray-green siltstones and mudstones interbedded with gray and gray-green glutenites and siltstones and is divided from bottom to top into the Xingezhuang, Jiangjunding, Jingangkou and Changwangpu formations (Hu et al., 2001). Yan and Chen (2005) obtained an isotope age of 73 Ma for the Jingangkou Formation (which they called the Hongtuya Formation) based on a basalt sample from the town of Daxizhuang in Jiaozhou City. All Laiyang hadrosauroids have been collected from the Jiangjunding and Jingangkou formations to date (Wang et al., 2010; Wang, Wang, et al., 2013).

Wiman (1929) described and erected *Tanius sinensis* based on a nearly complete skull and some postcranial bones from the Jiangjunding Formation collected by Tan (1923). Young (1958) subsequently named a new member of Lambeosaurinae, *Tsintaosaurus spinorhinus* and erected a second species of *Tanius*, *Ta. chingkankouensis*, based on material collected from the Jingangkou Formation. *Shantungosaurus giganteus* was described as a giant flat-head saurolophine, based on a nearly complete composite skeleton collected from Wangshi Group, in Longgujian,

Zhucheng, Shandong (Hu, 1973; Hu et al., 2001). Additionally, some specimens of *S. giganteus* found in Laiyang (Hu et al., 2001). The third species of *Tanius*, *Ta. laiyoungensis* was erected based on an ilium and a sacrum, collected from the same site as *Tsintaosaurus spinorhinus* and *Ta. chingkankouensis* (Zhen, 1976).

Laiyangosaurus youngi (Zhang et al., 2017) was erected as a new saurolophine hadrosaurid on the basis of several cranial elements from the Jingangkou Formation at a newfound bone bed in Laiyang. This new bone bed (Locality 2) is 1 km east to the Locality 1 where *Tsintaosaurus* was first found (Figure 1). Here, we thoroughly describe the postcranial elements of this taxon from Locality 2. These postcranial elements belong to five individuals in original description of *L. youngi* (Zhang et al., 2017). We provide additional postcranial characters to *L. youngi* and detailed comparative osteology with all other hadrosauroids from Laiyang.

2 | MATERIALS AND METHODS

2.1 | Materials

The specimens studied herein, are belong to five individuals of *Laiyangosaurus youngi* (two large ones and three small ones), which were collected from the same site (Locality 2) located in western of Jingangkou Village, Laiyang City, Shandong Province, and all are housed in the Institute of Vertebrate Paleontology and Paleoanthropology, Chinese Academy of Sciences, Beijing, China. The elements of each individual encapsulated within a small area, display typical saurolophine morphologies, and the same positional elements share similar features, so all these saurolophine bones can be assigned to *L. youngi*. The known long bones of the large individuals are almost twice as long as those of the small ones, hence, the whole size of the small individual is nearly half of that of the large ones. The length of the large composite skeleton of *L. youngi*, displayed in the museum of the Cretaceous National Geological Park of Laiyang Shandong, is 7.6 m, while the small one is 3.9 m (Figure 2).

2.2 | Phylogenetic analysis

We conducted a phylogenetic analysis of Hadrosoidea based on the matrix of Prieto-Márquez et al. (2016) to test the position of *Laiyangosaurus youngi* within hadrosaurid iguanodontians. The optimal tree (s) search was conducted in TNT version 1.1 (Goloboff et al., 2008). A heuristic search of 10,000 replicates using random

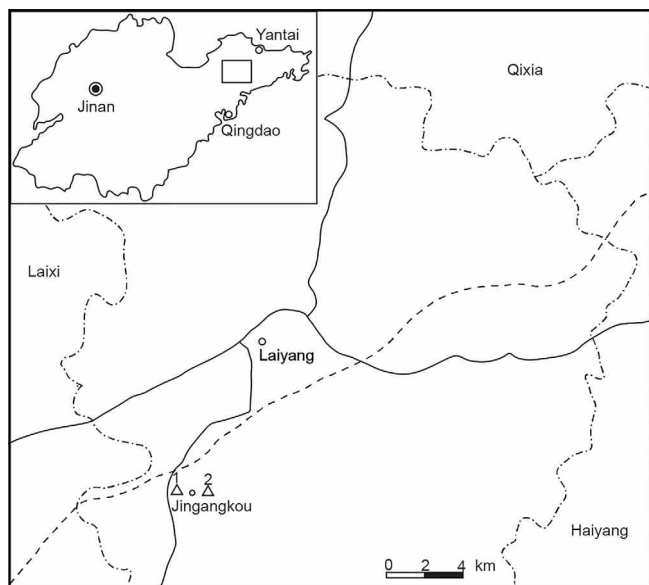


FIGURE 1 Localities map for *Laiyangosaurus youngi*. Locality 1 of *Tsintaosaurus spinorhinus* and locality 2 of *L. youngi* in Laiyang, Shandong, China (Modified from Wang et al., 2012).



FIGURE 2 Composite skeletons of *Laiyangosaurus youngi*. The large and small skeletons represent the adult and juvenile individuals respectively and are displayed in the museum of the Cretaceous National Geological Park of Laiyang Shandong.

addition sequences was performed, followed by branch swapping by tree bisection–reconnection holding 10 trees per replicate.

2.3 | Institutional abbreviations

BMNH, Beijing Museum of Natural History, Beijing, China; IVPP, Institute of Vertebrate Paleontology and Paleoanthropology, Chinese Academy of Sciences, Beijing, China.

3 | RESULTS

3.1 | Systematic paleontology

Ornithischia Seeley, 1887.
Ornithopoda Marsh, 1881.
Hadrosauroidea Cope, 1869.
Hadrosauridae Cope, 1869.

Saurolophinae Brown, 1914 (sensu Prieto-Márquez, 2010b).

Laiyangosaurus Zhang et al., 2017.

Laiyangosaurus youngi Zhang et al., 2017.

3.1.1 | Holotype

A large individual IVPP V 23401, including left maxilla, right squamosal, left dentary, axis, right scapula, left humerus, right ulna, left radius, right pubis, and right fibula, housed in the collection of the Institute of Vertebrate Paleontology and Paleoanthropology, Chinese Academy of Sciences, Beijing, China.

3.1.2 | Referred specimens

A small individual IVPP V 23402, including left maxilla, right premaxilla, right nasal, left squamosal, right and left dentaries, right and left surangulars, right sternum,

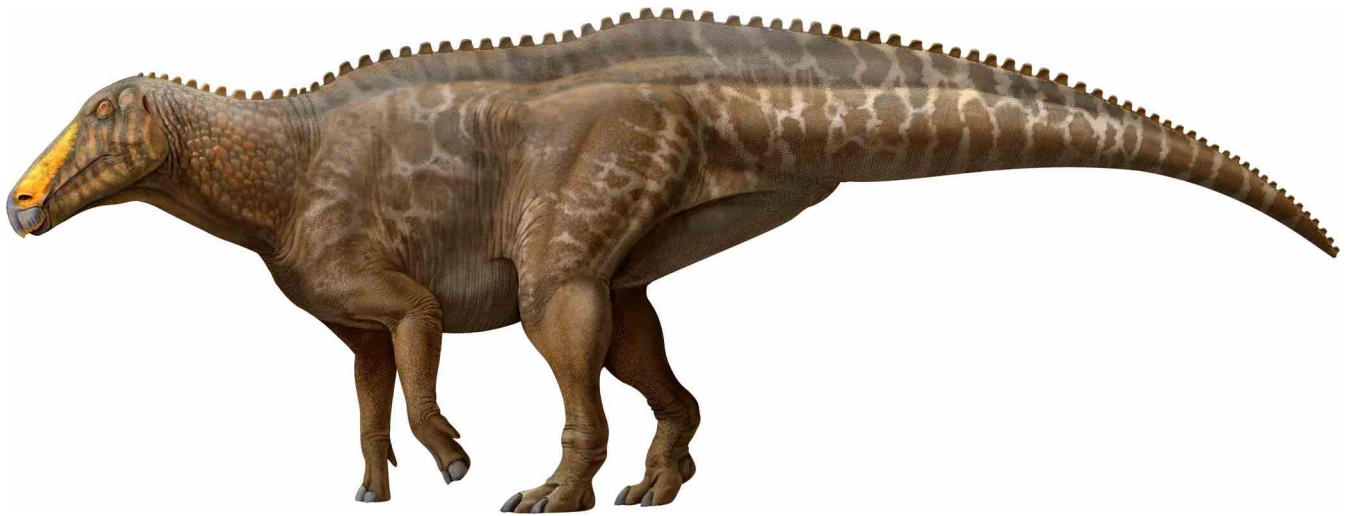


FIGURE 3 Life reconstruction of *Laiyangosaurus youngi*.

left coracoid, left scapula, right and left humeri, right ulna, left ilium, right pubis, right ischium, right and left femora, right and left tibiae, left fibula; a small individual IVPP V 23403, including right maxilla, left dentary, left surangular, left sternum, right scapula, left humerus, right ulna, left radius, right pubis; a large individual IVPP V 23404, including left dentary and sacrum; a small individual IVPP V 23405, including left maxilla, left jugal and left ilium.

3.1.3 | Locality and horizon

Locality 2, Jingangkou, Laiyang City, Shandong Province, China. Jingangkou Formation, Wangshi Group, Upper Cretaceous.

3.1.4 | Diagnosis

Laiyangosaurus youngi (Figure 3) is a sauropod distinguished by autapomorphies that include a prominent and narrow ridge on the lateral side of the nasal which forms the posterodorsal and posterior margin of the circumnasal depression, a primary ridge in most maxillary teeth slightly deflected posteriorly, a retroarticular process of the surangular that is dorsolatero-posteriorly recurved, and an orbital margin that is wider than the infratemporal margin of the jugal. *L. youngi* can be further distinguished by a number of unique character combinations that include a dorsal margin of nasal is flat, absence supracranial crest, a relatively shallow and rostro-dorsally directed caudal margin of the jugal lacrimal process, expanded anteroposteriorly as well as one or

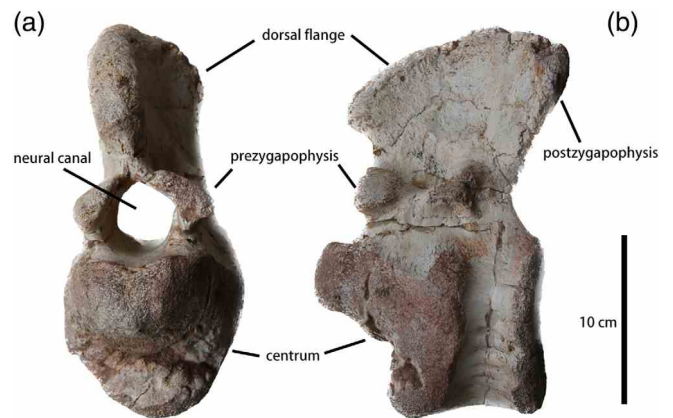


FIGURE 4 Axis (IVPP V 23401.4) of *Laiyangosaurus youngi*. In cranial (a) and left lateral (b) views.

more foramina on the rostral surface of the premaxilla, poorly expanded deltopectoral crest of the humerus, present a brevis shelf at the base of the postacetabular process of the ilium and a well-defined medioventral ridge on the medial side of the postacetabular process.

3.2 | Description

3.2.1 | Axis

The axis (IVPP V 23401.4) (Figure 4) is large and its centrum and the dorsal flange of the neural spine are preserved, but the postzygapophysis and diapophysis are damaged. The axis is opisthocoelous and has a small craniocaudal length. The dorsoventral height of the axis is approximately twice as long as its length. The centrum

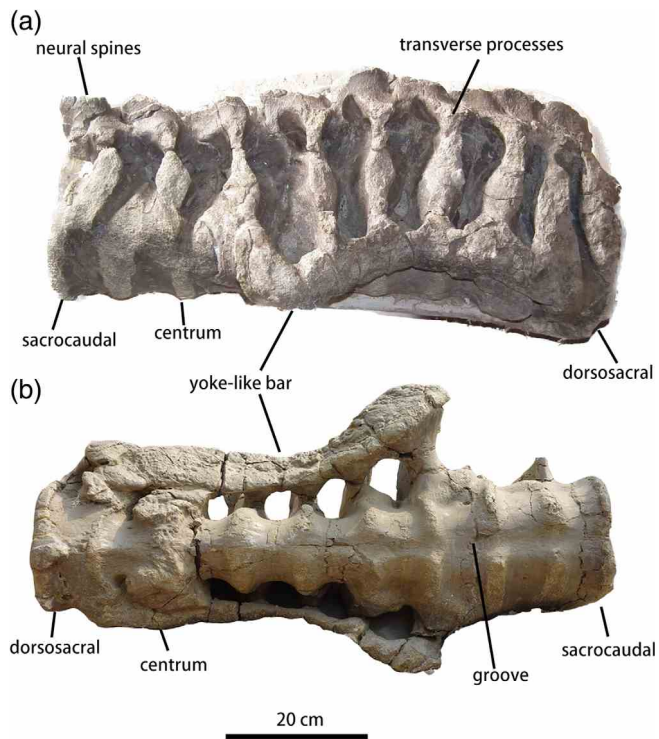


FIGURE 5 Sacrum (IVPP V 23404.2) of *Laiyangosaurus youngi*. In right lateral (a) and ventral (b) views.

is hourglass-shaped in lateral view, with a depression in the middle and multiple nutrient holes on the ventral side. There is a clearly protruding conical odontoid located at the dorsal half of the anterior part of the centrum. The neural spine has fused with the centrum dorsally, and the paired neural arch pedicels encircle an oval-shaped neural canal. A prominent prezygapophysis located at the craniolateral portion of each pedicel, with an oval, lightly eroded, dorsolaterally oriented articular facet. The prezygapophysis continuous with the heavily eroded diapophysis posterolaterally. The dorsally convex flange occupies the entire part of the neural spine. The dorsal margin of the flange starts from a hook-shaped cranial tip, and extends to the cranial most region of the postzygapophyses, without prominent embayment which separated the dorsal flange from the postzygapophyseal flange in *Brachylophosaurini* (Cuthbertson, 2006; Prieto-Márquez, 2014) and *Saurolophus* (Maryanska & Osmólska, 1984). The dorsal flange extends caudally with two heavily eroded postzygapophyses.

3.2.2 | Sacrum

The sacrum (IVPP V 23404.2) (Figure 5) consists of nine co-ossified sacral vertebrae, including one dorsosacral, seven true sacrals, and one sacrocaudal, while the neural

spines of all the sacrum are not preserved. The preserved proximal part of the neural spines shows that they are laminae and slightly caudodorsally extend. The horizontal and robust transverse processes expanded laterally from the base of the neural arches, forming a sub triangle in cross section. A bony lamina extends ventrally from the base of each transverse process. The laminae of the cranial six sacral vertebrae fuse with a robust and sinuous yoke-like bar that extends longitudinally at base of the centra. However, the lamina of the last sacral vertebra is not involved in the composition of the bar, as in *Shantungosaurus* and *Tsintaosaurus*. The yoke-like bar is gently dorsally convex in lateral view and laterally curved along its caudal half in ventral view. The centrum of the dorsosacral vertebra is relatively robust, and its cranial articular surface is heart shaped. In contrast to the dorsosacral, the following four sacrals are relatively slender, however, the last three sacrals and the sacrocaudal vertebra have particularly larger centra. The centrum of the sacrocaudal vertebra is mediolaterally wide with a sub hexagon caudal articular surface. A groove extends ventrally along the last seven centra, while a convex occurs in the ventral surface of the two carinal sacrals.

3.2.3 | Sternum

Two sterna of two small individuals, the left one (IVPP V 23403.4) (Figure 6a, b) and the right one (IVPP V 23402.9) (Figure 6c) are nearly complete, only partially missing the craniomedial blade of IVPP V 23402.9. The sterna are hatchet-shaped and dorsoventrally compressed, as in other hadrosaurids, with a flattened dorsal surface and a convex ventral surface. The handle-shaped caudolateral process of the sternum is longer than the craniomedial blade, as in most hadrosaurids, but in contrast to *Amurosaurus* (Godefroit et al., 2004), *Tsintaosaurus* (Young, 1958), and most non-hadrosaurid hadrosauroids. The distal end of the caudolateral process is rough and slightly expanded. The craniomedial blade is quadrilateral and thicker at its middle portion, with a small medial process projected from the caudomedial corner of the craniomedial blade, as in *Edmontosaurus* (Prieto-Márquez, 2008). The proximal borders of the craniomedial blade are rough in both dorsal and ventral surfaces, and the lateral border is slightly concave.

3.2.4 | Coracoid

One small right coracoid (IVPP V 23402.10) (Figure 6d, e) is nearly completely preserved and formed by a quadrangular mediolaterally compressed central body. The

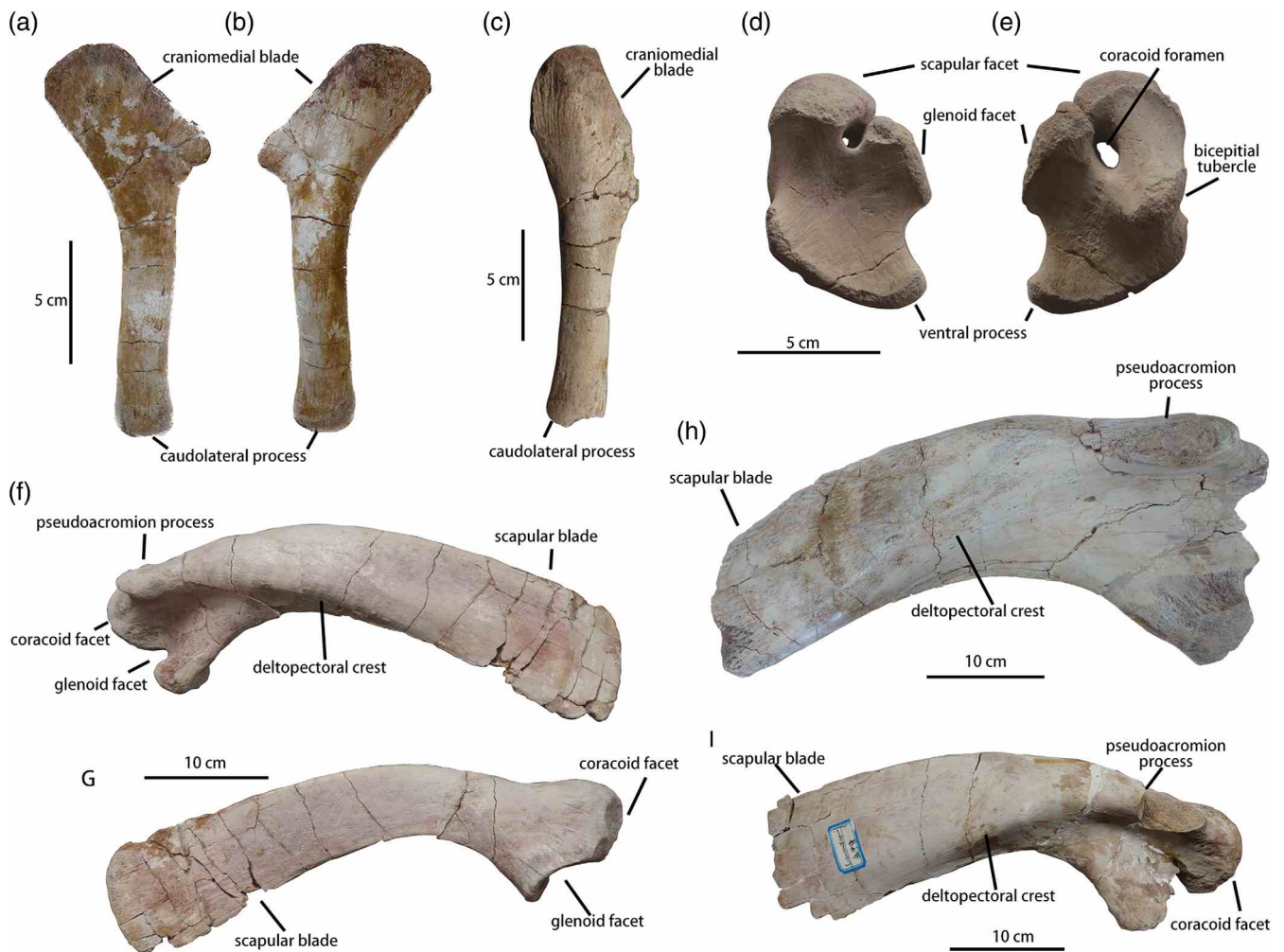


FIGURE 6 Pectoral girdles of *Laiyangosaurus youngi*. (a) and (b), left sternum (IVPP V 23403.4) in ventral (a) and dorsal (b) views; C, right sternum (IVPP V 23402.9) in dorsal view; (d) and (e), right coracoid (IVPP V 23402.10) in medial (d) and lateral (e) views; (f) and (g), left scapula (IVPP V 23403.5) in lateral (f) and medial (g) views; (h), right scapula (IVPP V 23401.5) in lateral view; (i), right scapula (IVPP V 23402.11) in lateral view.

glenoid and scapular facet occupy its ventral part, and the biceps tubercle and ventral process are in the dorsal half. In lateral view, the angle between the glenoid and scapular facets are more than 120° , which is different from most members of the Hadrosauridae but is more similar to the non-hadrosaurid hadrosauroids (Prieto-Márquez, 2008). However, the larger angle between the glenoid and scapular facet in the small coracoids of *Laiyangosaurus* may be due to ontogeny, because the same feature varied greatly in both adult and juvenile individuals of *Bactrosaurus johnsoni* (Gilmore, 1933; Prieto-Márquez, 2011). Both the glenoid and the scapular facet are slightly concave, with the glenoid being D-shaped and the scapular facet being approximately circular. The lateral margin of the scapular facet is nearly three-quarters of the breadth of the lateral margin of the glenoid facet. The oval coracoid foramen penetrates the coracoid mediolaterally at the

connection between the glenoid and the scapular facets. The coracoid foramen is not closed in IVPP V 23402.10, and a narrow groove is present between the glenoid and the scapular facets. Whether the coracoid foramen is completely closed is an important ontogenetic feature (Brett-Surman & Wagner, 2006; Prieto-Márquez, 2014).

The craniomedial margin of the coracoid is concave, and associated to a relatively robust and anterodorsally extended bicipital tubercle, which is similar to hadrosaurids (Prieto-Márquez, 2008). There is a distinct notch between the bicipital tubercle and the ventral process in the medial view. The hook-shaped ventral process is mediolaterally compressed and posteroventrally recurved, which is similar to hadrosaurids (Prieto-Márquez, 2008). However, the ventral process is relatively short dorsoventrally, which may also be due to ontogeny (Brett-Surman & Wagner, 2006; Prieto-Márquez, 2014).

3.2.5 | Scapula

There are one large right scapula (IVPP V 23401.5) (Figure 6h) and two small scapulae, a right one (IVPP V 23402.11) (Figure 6i) and a left one (IVPP V 23403.5) (Figure 6f, g). The small scapulae are nearly completely preserved, while the large ones only preserved the proximal region. The scapula is mediolaterally compressed plate-shaped and its dorsal margin is curved. In the medial view, the surface of the scapula is mostly flat. However, the lateral surface gently convex from the proximal constriction through most of the length of the scapular distal blade. The proximal region is mediolaterally thicker, with the coracoid facet and the glenoid. The coracoid facet is oval and slightly concave, located on the dorsal half, while the glenoid is located ventrally and also slightly concave, forming a narrow crescent-shaped articulation surface. The glenoid is elongated and extends ventrolaterally and terminates in a prominently laterally projected ventral corner. The coracoid facet extremely extends cranially, similar to *Gryposaurus* (Lambe, 1914), *Prosaurolophus* (Brown, 1916), *Secernosaurus* (Brett-Surman, 1979), and *Willinaqake* (Juárez Valieri et al., 2010) (Prieto-Márquez, 2008, 2010b). Between the proximal region and the distal blade, the scapular neck is dorsoventrally constricted.

The robust and laterally projected pseudoacromion process extends nearly horizontally, similar to saurolophines, but different from non-hadrosaurid hadrosauroids and lambeosaurines with a dorsally curved cranial end of the pseudoacromion process (Prieto-Márquez, 2008, 2010b). In lateral view, the pseudoacromion process forms the dorsal edge of the proximal region of the scapula, and between the pseudoacromion process and the glenoid, there is a deep triangular depression that occupies most of the lateral surface of the proximal region of the scapula.

The deltopectoral crest is well-developed and extends obliquely from the posteroventral margin of the pseudoacromion process to the ventral margin of the scapular blade. The dorsal and ventral edges of the distal scapular blade are curved ventrally, and the distal region of the blade is gradually extended dorsoventrally.

3.2.6 | Humerus

There are four humeri, the proximal region of a large left one (IVPP V 23401.6) (Figure 7a, b) and three nearly complete small ones (IVPP V 23402.12, IVPP V 23402.13, and IVPP V 23403.6) (Figure 7c–f). The articular head of the humerus is massive, rounded, and has a triangular cross-section. The medial surface of the proximal half of the humerus is concave and the lateral surface is convex

forming a thick and rugose central ridge. The deltopectoral crest projects lateroventrally from the head and extends along the proximal half of the bone. Similar to other hadrosaurids, the deltopectoral crest is relatively long. The length of the deltopectoral crest is significantly greater than that of the humeral shaft. The anteroposteriorly width of the humerus is relatively small, similar to *Brachylophosaurus* (Prieto-Márquez, 2007) and non-hadrosaurid hadrosauroids (Prieto-Márquez, 2008, 2010b). The width of humerus increases gradually distally, reaching the greatest at the ventral corner of the deltopectoral crest. In lateral view, the angle between the anterolateral edge of the deltopectoral crest and its distal edge ranges from 121° to 129°, similar to that of *Taninus* (Wiman, 1929), *Bactrosaurus* (Gilmore, 1933; Prieto-Márquez, 2011), *Brachylophosaurus* (Prieto-Márquez, 2007), and *Edmontosaurus* (Prieto-Márquez, 2014).

The humeral shaft is mediolaterally thick and almost cylindrical, which forms the distal half of the humerus with the lateral radial and medial ulnar condyles. The ulnar condyle is larger than the radial one. The condyles are separated by a deep notch for reception of the olecranon process of the ulna.

3.2.7 | Ulna

One large right ulna (IVPP V 23401.7) (Figure 7g, h) and two small right ulnae (IVPP V 23402.14 and IVPP V 23403.7) (Figure 7i, j) are nearly completely preserved. The ulnae are rod-shaped; the proximal and distal ends are both expanded. The proximal cross-section of the ulna is triangular, with a prominent olecranon as the posterior apex and two anteriorly extended flanges as the two sides of the triangular. The olecranon is subconical and points dorsally. The medial flange extends anteromedially and is larger than the anterolaterally extended flange. Between the two flanges, there is a wide notch for reception of the proximal region of the radius. In the lateral view, the ulna appears S-shaped, with the proximal region bent forward and the distal region bent backward. The ulna tapers distally, while the distal end is slightly expanded. The distal cross-section of the ulna is also triangular, but the apex of this triangle points anterolaterally. There is a narrow and rough distal radial facet on the anteromedial surface of the distal end.

3.2.8 | Radius

There are two complete radii a large left one (IVPP V 23401.8) (Figure 7k, l) and a small left one (IVPP

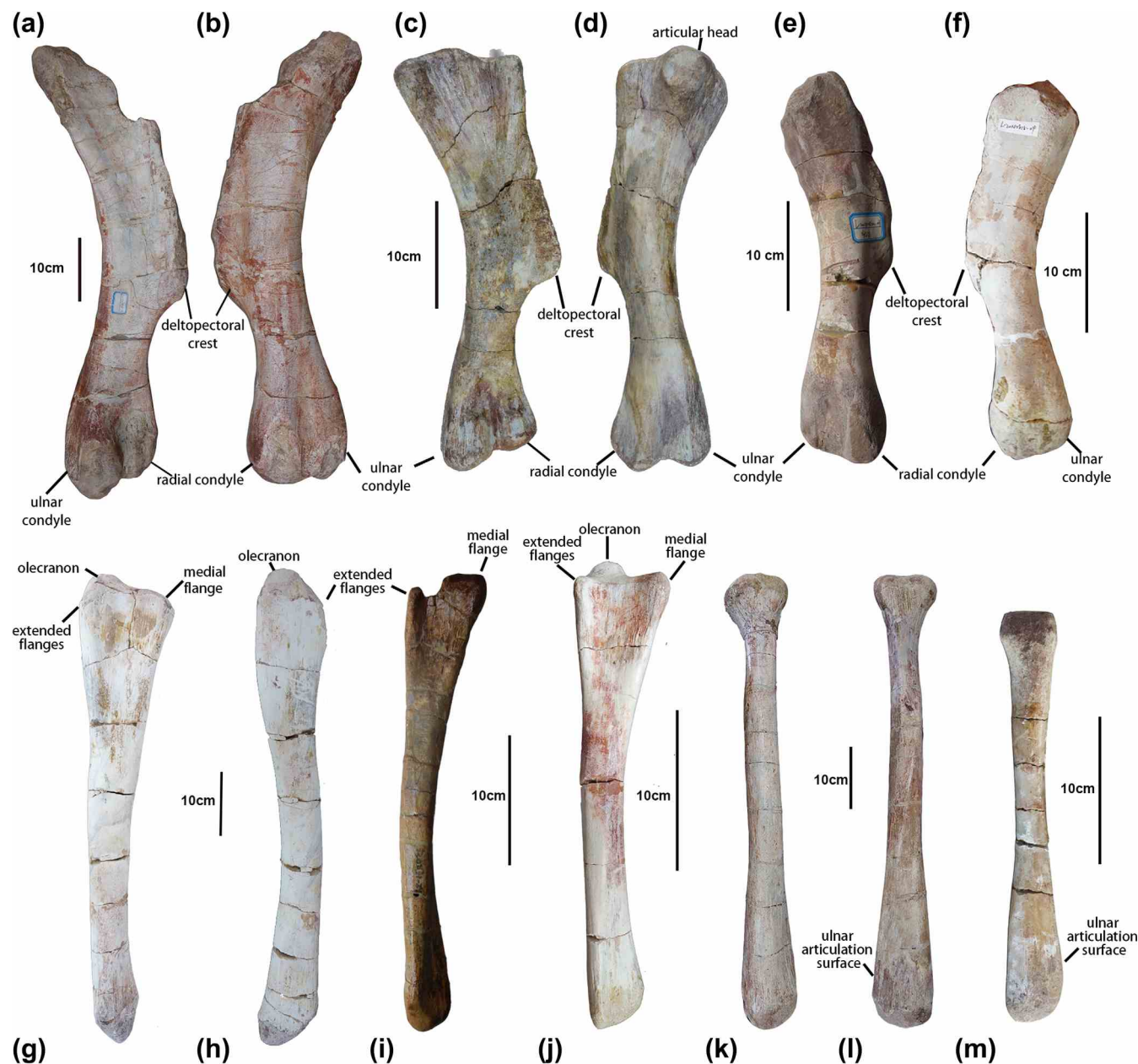


FIGURE 7 Forelimbs of *Laiyangosaurus youngi*. (a) and (b), left humerus (IVPP V 23401.6) in medial (a) and lateral (b) views; (c) and (d), left humerus (IVPP V 23402.13) in medial (c) and lateral (d) views; (e), right humerus (IVPP V 23402.12) in lateral view; (f), left humerus (IVPP V 23403.6) in lateral view; (g) and (h), right ulna (IVPP V 23401.7) in cranial (g) and lateral (h) views; (i), right ulna (IVPP V 23402.14) in cranial view; (j), right ulna (IVPP V 23403.7) in cranial view; (k) and (l), left radius (IVPP V 23401.8) in cranial (k) and caudal (l) views; (m), right radius (IVPP V 23403.8) in caudal view.

V 23403.8) (Figure 7m). The radii are thin rod-shaped, with slightly expanded proximal and distal ends. The proximal expansion is significant and abrupt, with a flattened proximal surface. In the posterior view, a rough longitudinal ridge extends on the proximal region to fit into the proximal notch of the ulna. The shaft of the radius gradually expands distally. A narrow ulnar articulation surface faces posterolaterally in the distal region of the radius.

3.2.9 | Ilium

There are two small left partial ilia, one (IVPP V 23402.15) (Figure 8a, b) lacks the preacetabular process and the pubic peduncles, and the other (IVPP V23405.3) (Figure 8c) lacks anterior part of the preacetabular process and the supraacetabular process. The preserved preacetabular processes of ilia are narrow and elongated. The lateromedially compressed preacetabular process is

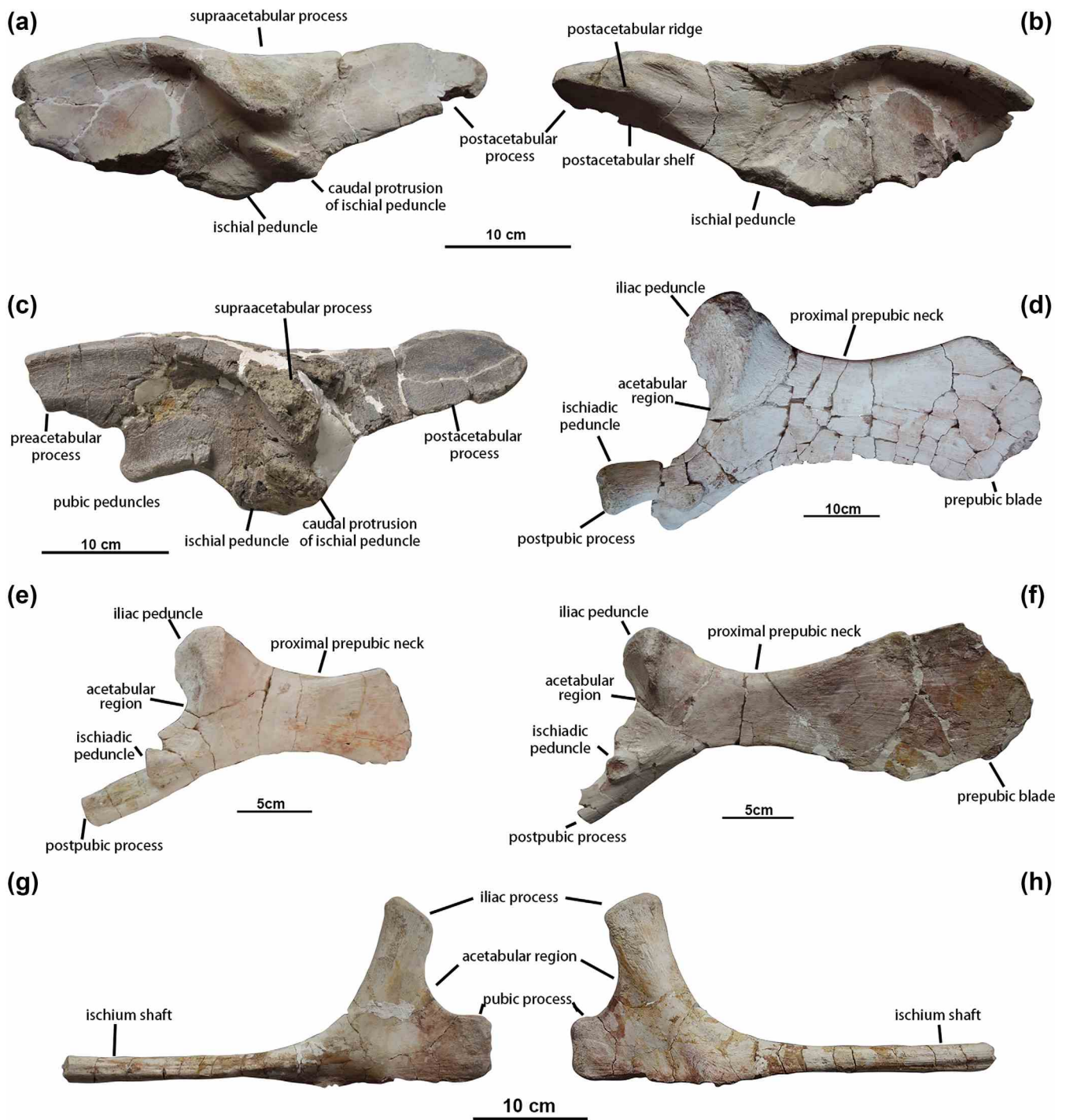


FIGURE 8 Pelvic girdles of *Laiyangosaurus youngi*. (a) and (b), left ilium (IVPP V 23402.15) in lateral (a) and medial (b) views; (c), left ilium (IVPP V 23405.3) in lateral view; (d), right pubis (IVPP V 23401.9) in lateral view; (e), right pubis (IVPP V 23403.9) in lateral view; (f), right pubis (IVPP V 23402.16) in lateral view; (g) and (h), right ischium (IVPP V 23402.17) in lateral (g) and medial (h) views.

deflected anteroventrally, forming an angle of 160° with the anteroposterior axis of the central plate, similar to the non-hadrosaurid hadrosauroids, but different from the lower preacetabular process of the hadrosaurids (Prieto-Márquez, 2008, 2010b). However, the degree of ventral curvature of the preacetabular process of the

ilium increase would be an ontogenetic feature (Mori et al., 2015; Prieto-Márquez, 2014). In the medial view, a large ridge extends from the dorsal margin of the preacetabular process to the central plate of the ilium. In the dorsal view, the preacetabular process is slightly curved laterally.

The central plate of the ilium is lateromedially compressed, and its dorsoventral height is about 70%–75% of the anteroposterior length, similar to other hadrosaurids (Prieto-Márquez, 2008, 2010b). The prominent supraacetabular process extends along the dorsal margin of the central plate and projects lateroventrally. The supraacetabular process is long, its anteroposterior length is about 70% of that of the central plate. The ventral apex of supraacetabular process reaches the half depth of the central plate, but not below the level of the ventral margin of the proximal region of the postacetabular process. The ventral margin of the central plate forms the roof of the acetabulum. The slender pubic peduncle forms the anteroventral corner of the central plate, and the rostroventral part of the central plate is the robust ischiadic peduncle, which formed by two small protrusions. The caudal-most one located caudoventrally of the supraacetabular process, as most hadrosaurids (Prieto-Márquez, 2008, 2010b).

The postacetabular process of the ilium appears nearly rectangular in lateral view, with the dorsal and ventral edges parallel and converging at the posterior end, forming a rounded posterior edge. The lateral surface of the postacetabular process is concave. There is a brevis shelf at the base of the postacetabular process of the ilium and a well-defined medioventral ridge on the medial side of the postacetabular process, similar to *Secernosaurus* (Brett-Surman, 1979).

3.2.10 | Pubis

There are one large right pubis (IVPP V 23401.9) (Figure 8d) and two small right pubes (IVPP V 23402.16 and IVPP V 23403.9). One (IVPP V 23403.9) (Figure 8e) lacks the distal part of the prepubic blade, and another (IVPP V 23402.16) (Figure 8f) lacks the ischiadic peduncle. The pubis consists of a cranial blade-like prepubic process and three caudal projections containing the iliac and ischiadic peduncles, and an elongated postpubic process. The prepubic process is composed of a paddle-shaped distal prepubic blade and a dorsoventrally constricted proximal prepubic neck. The prepubic process is relatively short, with the preserved anteroposterior length about 2.5 times the depth. The prepubic blade of a small pubis (IVPP V 23402.16) is nearly completely preserved, only the distal margin has some abrasions. This prepubic blade distally expands more dorsally than ventrally. The prepubic neck is narrow and long, about half as deep as the distal blade, but longer than the prepubic blade. The concavity of the dorsal margin of prepubic neck is symmetric with the concavity of the ventral margin. The maximum depth of the prepubic blade is slightly deeper than the maximum breadth of the acetabular margin.

The prepubic neck is caudally continuous with the proximal rest of the pubis. The iliac peduncle projects caudodorsally from the dorsal portion of the acetabular region of the pubis. The tetrahedral iliac peduncle is ventrally linked to the ischiadic peduncle by the cranially concave acetabular margin of the pubis. The slender ischiadic peduncle is mediolaterally compressed and projects caudoventrally with laterally offsetting from the post public process. There is a prominent protuberance at the cranioventral portion of the ischiadic peduncle of the large pubis (IVPP V 23401.9), which does not exist in the small one (IVPP V 23402.16). The rest of the postpubic process shows it would be long rodlike, and extend caudoventrally. The postpubic process is medial to, and slightly more ventrally oriented than the ischiadic peduncle.

3.2.11 | Ischium

One small right ischium (IVPP V 23402.17) (Figure 8g, h) with the proximal plate and the proximal portion of the ischium shaft preserved, missing the obturator process and distal end of the ischium shaft. Two additional ischia are included: L2-130810, preserves the obturator process, but slightly larger, and no other materials could match its size; a large ischium preserves the complete ischium shaft, but have not collected. The proximal plate is compressed lateromedially and has slightly lateral diversion at the most proximal end. The iliac process is subrectangular and extends craniodorsally from the dorsal region of the proximal plate. Its caudodorsal margin is straight without the caudally recurved apex as saurolophine hadrosaurids (Prieto-Márquez, 2008, 2010b), and its cranioventral margin are ventrally continuous with the dorsal margin of the pubic process forming the acetabular margin of the ischium. The pubic process is also subrectangular, but extending cranially shorter and dorsoventrally deeper. The caudoventrally extended corner of the pubic process and the ventrally projected obturator process form a narrow and ventrally opened obturator gutter. The long rod-shaped ischial shaft extends caudally from the position of the obturator process, and shows a rounded distal end as saurolophine hadrosaurids, without the ventrally curved foot-like process in basal hadrosaurids and lambeosaurine hadrosaurids (Prieto-Márquez, 2008, 2010b).

3.2.12 | Femur

Two small femora were preserved: the left one (IVPP V 23402.19) (Figure 9a, b) is nearly complete, and the right one (IVPP V 23402.18) (Figure 9c) lacks the greater trochanter and the distal portion. The femur has a long and

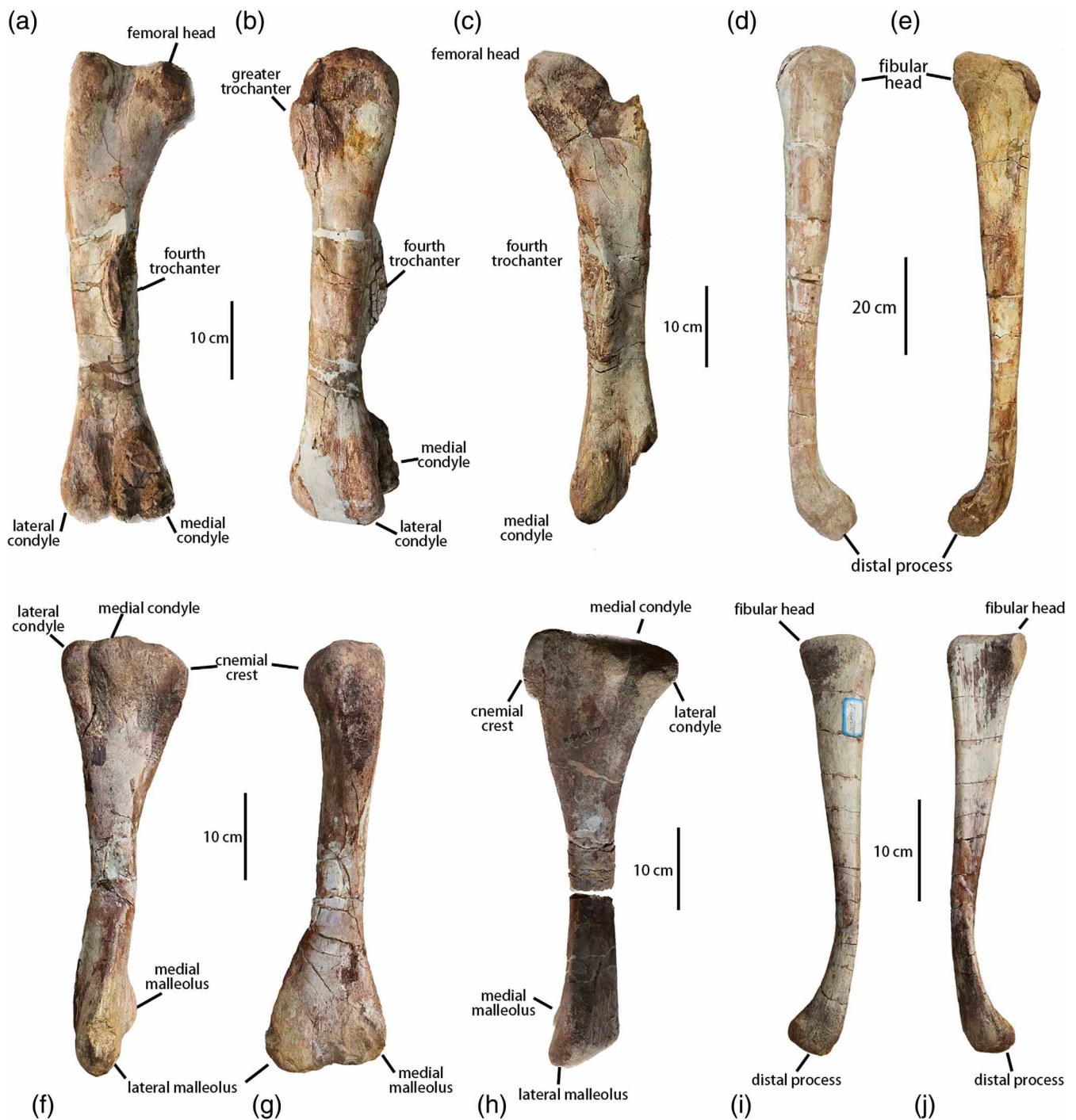


FIGURE 9 Hindlimbs of *Laiyangosaurus youngi*. (a) and (b), left femur (IVPP V 23402.19) in caudal (a) and lateral (b) views; (c), right femur (IVPP V 23402.18) in caudal view; (d) and (e), right fibula (IVPP V 23401.10) in lateral (d) and medial (e) views; (f) and (g), right tibia (IVPP V 23402.20) in lateral (f) and cranial (g) views; (h), left tibia (IVPP V 23402.21) in lateral view; (i) and (j), left fibula (IVPP V 23402.22) in lateral (i) and medial (j) views.

thick cylindrical shaft, with two expanded ends. The proximal portion of the femur is mediolaterally expanded, with a prominent subcylindrical femoral head projecting medially. The femoral head is separated from the greater trochanter, the lateral part of the proximal end of the femur, by a shallow groove. There is a wedge-

shaped lesser trochanter separated from the greater trochanter cranioventrally by a cleft. In the middle of the caudal surface of femoral shaft, there is a triangle fourth trochanter. The fourth trochanter is long and flat, about one-fourth of the total length of the femur. The distal portion of the femur expands craniocaudally, especially

more caudally, and is mediolaterally divided into two condyles by a narrow and deep intercondylar groove. The condyles are both mediolaterally compressed, but the medial condyle is larger and mediolaterally thicker than the lateral one.

3.2.13 | Tibia

Two small tibiae (IVPP V 23402.20 and IVPP V 23402.21) (Figure 9f–h) are nearly completely preserved. The tibia is a robust and cylindrical central shaft, with expanding proximally and distally. The proximal end expands craniocaudally, with slight mediolaterally compression in the proximal half of the shaft. Caudally, the proximal end has two small condyles, which project laterally and are separated by a narrow cleft. While cranially, a large cnemial crest extends cranioventrally, nearly forming the cranial margin of the proximal half of the shaft. On the lateral surface of the cnemial crest, there is a shallow depression for accepting the proximal end of the fibula. The distal region expands mediolaterally and slightly compresses craniocaudally. The distal end of the tibia has medial and lateral malleoli, separated by a wide groove.

3.2.14 | Fibula

One large right fibula (IVPP V 23401.10) (Figure 9d, e) and one small left fibula (IVPP V 23402.22) (Figure 9i, j) are nearly completely preserved. The fibula is slender and mediolaterally compressed, and craniocaudally expands proximally and distally. The proximal end expands larger and more abruptly than the distal end. In the proximal half of the shaft, the lateral surface of the fibula is convex, while the medial surface is concave for the reception of the proximal portion of the tibia. The fibular shaft twists medially along the distal third, and also has a medial triangular joint surface for the distal end of tibia. The distal end of the fibula protrudes cranially and forms a prominent clublike structure.

3.3 | Phylogenetic analysis

We conducted a maximum parsimony analysis to assess the phylogenetic position of *Laiyangosaurus youngi* within hadrosauroid iguanodontians. This analysis is based on the 273-character matrix of Prieto-Márquez et al. (2016), consisting of 189 cranial and 84 postcranial equally weighted characters (see Appendix A for character states of *L. youngi*). The new matrix is consisted of 62 hadrosauroid species (including 16 outgroups to

Hadrosauridae, 23 saurolophines, and 21 lambeosaurines). Prieto-Márquez (2014) suggested that the ontogeny would affect the phylogenetic relationships of saurolophine hadrosaurids. Therefore, we exclude the juvenile state of ontogenetically variable characters of *L. youngi* in the matrix, including degree of curvature of the caudal margin of the quadrate (107), ratio between the length of the lateral margin of the facet for the scapular articulation and the length of the lateral margin of the glenoid (198), development of the “hook-like” ventral process of the coracoid, measured as the ratio between the dorsoventral depth and the breadth of the process (201), development of the lateroventral projection of the supraacetabular crest of the ilium (228), craniocaudal breadth of the supraacetabular process (229).

The analysis resulted in 16 most parsimonious trees of 1008 steps each (Consistency Index 0.395, Retention Index 0.778). The strict consensus tree shows that *L. youngi* is in Saurolophinae, which is in consistent with the result of our anatomical comparison (Figure 10). This analysis also shows that *L. youngi* lies in a monophyletic group, which is known as Edmontosaurini, supported by four synapomorphies: present a ridge bordering the caudodorsal margin of the circumnarial depression (character 75 [1,2]), maxilla-lacrima contact largely covered externally by the jugal-premaxilla contact (character 86 [1], convergent in the brachylophosaurine clade), invaginated caudal region of the circumnarial fossa (character 171 [2]), and absence supracranial crest (character 173 [0], convergent in *Acristavus* and non-Saurolophidae Hadrosauriformes except *Lophorhothon*).

The position of *L. youngi* within Edmontosaurini is not well resolved, but this taxon can still be distinguished from others in this clade on the basis of seven autapomorphies: 33–4 tooth positions in the maxillary dental battery (character 11 [1]), maxillary battery contains a mixture of teeth with primary ridge positioned caudally and teeth with the ridge at the center of the crown (character 14 [0]), retroarticular process of the surangular laterally recurved (character 43 [1]), one or more foramina on the rostral surface of the premaxilla (character 61 [1]), relatively shallow dorsoventral expansion of the caudal margin of the lacrimal process of the jugal, rostrorodorsally directed and forming little of the rostrorodorsal margin of the orbital rim (character 97 [0]), medial articular surface of the rostral process of the jugal deep concavity roofed by an oblique (rostrorodorsally oriented) narrow shelf (character 100 [1]), and a wider orbital margin and relatively constricted ventral margin of the infratemporal fenestra (character 106 [2]), poorly expanded deltopectoral crest of the humerus (character 212 [11]), brevis shelf at the base of the postacetabular process of the ilium (character 236 [1]), Medioventral ridge on the medial side

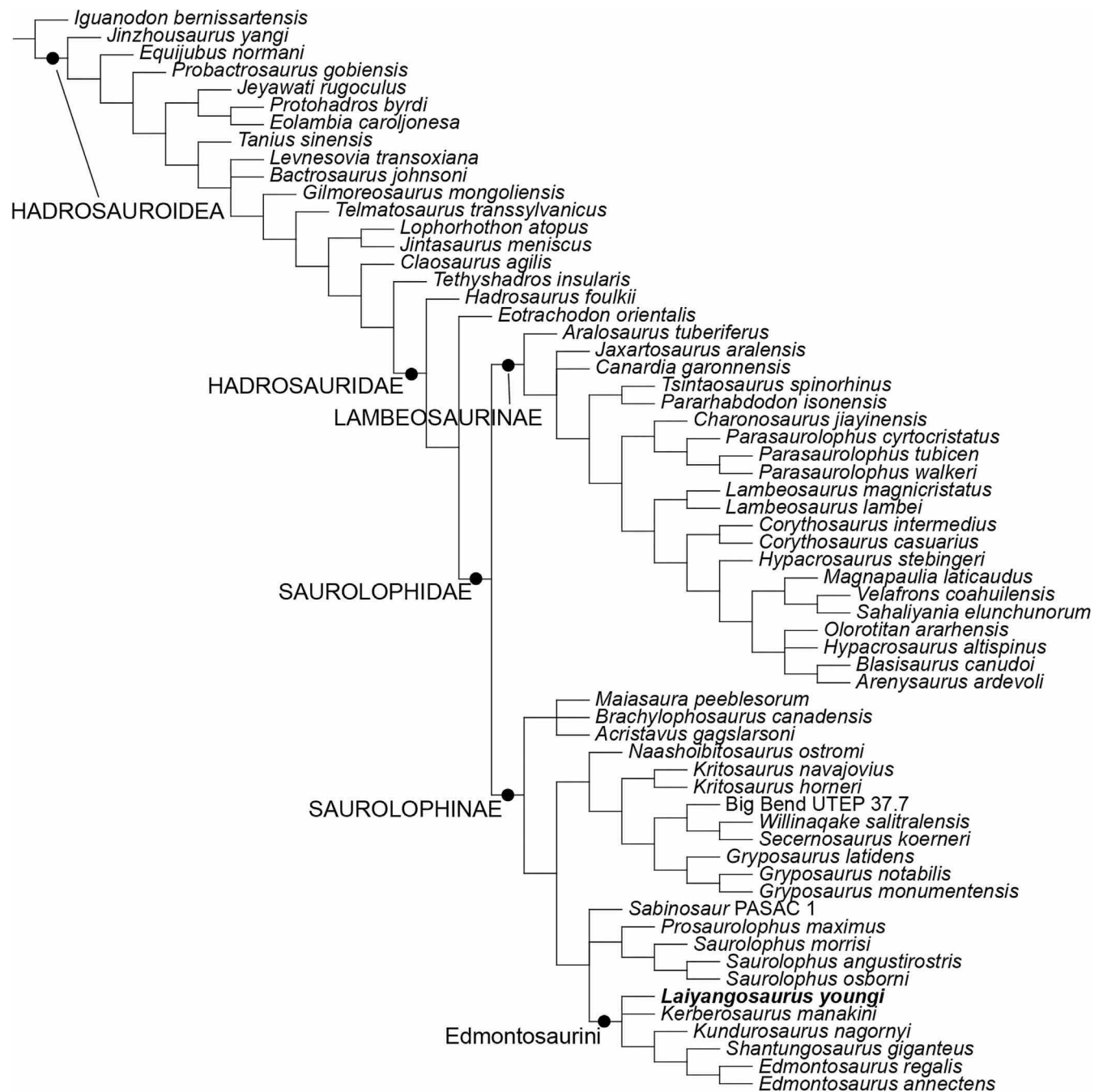


FIGURE 10 Strict consensus tree of the 16 most parsimonious trees resulting from the phylogenetic analysis of hadrosauroid relationships, showing the position of *Laiyangosaurus youngi*.

of the postacetabular process, crossing the bone surface from the proximoventral to the caudodorsal margins and orientation of the brevis shelf (character 237 [2]).

4 | DISCUSSION

There are three genera of hadrosauroids reported from Laiyang, *Tanius* (Wiman, 1929), *Tsintaosaurus* (Young, 1958), and *Shantungosaurus* (Hu, 1973). *Tanius* has three

species reported, the type species *Ta. sinensis* was assigned to the non-hadrosaurid hadrosauroids in recent phylogenetic analyses (Prieto-Márquez, 2010b; Xing, Wang, et al., 2014). The other two species, *Ta. chingankouensis* (Young, 1958), and *Ta. laiyangensis* (Zhen, 1976) are known only from postcranial skeletons, which show several hadrosaurid characters, so their validity was doubted (Buffetaut & Tong, 1993, 1995; Horner et al., 2004; Zhang et al., 2019). Zhang et al. (2017) compared *Laiyangosaurus* with *Ta. sinensis* for the

cranial materials, and *Laiyangosaurus* shows a series of hadrosaurid characteristics, which distinguished it from *Ta. sinensis* and other non-hadrosaurid hadrosauroids. Our study here reveals that the postcranial skeletons of *Laiyangosaurus* also display a suite of typical hadrosaurid characters. The distal region of the scapular blade of *Laiyangosaurus* is dorsoventrally expanded, while the dorsal and ventral margins are horizontal at the distal region of the scapular blade of *Ta. sinensis*. *Laiyangosaurus* has a relatively longer deltopectoral crest of the humerus than *Ta. sinensis*. The apex of the ventral margin of the supraacetabular crest is located craniodorsally to the caudal protuberance of the ischiadic peduncle of the ilium in *Laiyangosaurus*, while caudodorsally in *Ta. sinensis*. In addition, the coracoid of *Laiyangosaurus* has a concave craniomedial margin, a relatively large biceps tubercle, and a recurved ventral “hook-like” process, which is distinguished *Laiyangosaurus* from the non-hadrosaurid hadrosauroids.

Tsintaosaurus spinorhinus is one of the well-known Asian lambeosaurine, including a nearly complete composite skeleton, an incomplete skull, and additional postcranial material recovered from the bone bed of locality 1 in Laiyang. The cranial material comparison shows there are some significant differences between *Laiyangosaurus* with *Tsintaosaurus* (Zhang et al., 2017), while postcranial skeletons of *Laiyangosaurus* also can be easily distinguished from *Tsintaosaurus* and other lambeosaurines by some typical saurolophine features. The pseudoacromion process of the scapula of *Laiyangosaurus* is horizontal, while the cranial region of the pseudoacromion process is dorsally recurved in *Tsintaosaurus*. *Laiyangosaurus* has a well development of the deltoid ridge of the scapula, the ventral margin of the deltoid ridge reaches the ventral margin of the scapula, but in *Tsintaosaurus*, the deltoid ridge only weakly develops in the proximal region of the scapula, with a poorly demarcated ventral margin. The deltopectoral crest of the humerus is relatively shorter in *Laiyangosaurus* than that in *Tsintaosaurus*. *Laiyangosaurus* has a rounded the distal margin of the iliac peduncle of the ischium, without the thumb-like iliac peduncle, which strongly reversed in the caudodorsal corner. The pubic peduncle of the ischium of *Laiyangosaurus* is short, parallel to the ischial shaft, and the dorsal acetabular margin of the pubic peduncle is higher than the dorsal margin of the ischial shaft, while it is relatively longer, slightly inclined ventrally, and at the same level as the dorsal margin of the ischial shaft in *Tsintaosaurus*. The distal region of the ischial shaft is slightly expanded into a blunt end in *Laiyangosaurus*, unlike in ventrally *Tsintaosaurus* expanded forming a large “foot” process.

Shantungosaurus was named by Hu (1973) as a member of Saurolophinae, based on a nearly complete skeleton from the Upper Cretaceous Wangshi Group of Zhucheng, while some elements were also found in Laiyang (Hu et al., 2001). *Laiyangosaurus* and *Shantungosaurus* share some important cranial characteristics and have some differences (Zhang et al., 2017). Our anatomical examinations reveal that the postcranial materials of *Laiyangosaurus* and *Shantungosaurus* also share some typical saurolophine characters, which are described above for distinguished with *Tsintaosaurus*. However, *Laiyangosaurus* still has some differences with *Shantungosaurus* and other members of Edmontosaurini, *Edmontosaurus regalis* (Lambe, 1917), *E. annectens* (Marsh, 1892), *Kerberosaurus* (Bolotsky and Godefroit, 2004) and *Kundurosaurus* (Godefroit et al., 2012). *Laiyangosaurus* has a relatively long craniodorsal region of scapula (ratio between the distance from the coracoid joint and the cranial end of the pseudoacromion process and the height between this and the ventral apex of the glenoidal facet more than 0.45, Prieto-Márquez, 2010b), which is similar to *Kundurosaurus*, but different from other members of Edmontosaurini. The poorly expanded deltopectoral crest of the humerus (ratio between the width of the humerus across the distal fourth of the deltopectoral crest and the width of the distal shaft at the point of maximum curvature less than 1.65, Prieto-Márquez, 2010b) of *Laiyangosaurus* is distinguished from that of *Shantungosaurus* and *Edmontosaurus*. There is a brevis shelf at the base of the postacetabular process of the ilium and a well-defined medioventral ridge on the medial side of the postacetabular process, which are different from all the other members of Edmontosaurini, but similar to *Secernosaurus* (Brett-Surman, 1979), *Tsintaosaurus* and *Tanius*.

Ta. chingkankouensis (Young, 1958) and *Ta. laiyangensis* (Zhen, 1976) were erected based on a few postcranial bones collected in the same excavation with *Ts. spinorhins* at Jingangkou, Laiyang (Location 1). Buffetaut and Tong (1993) considered that *Ta. chingkankouensis* shows advanced hadrosaurid features of the ilium, and would not belong to the genus *Tanius*. Horner et al. (2004) regarded *Ta. chingkankouensis* as a junior synonym of *Ta. sinensis* and *Ta. laiyangensis* as a junior synonym of *Ts. spinorhinus*. Zhang et al. (2019) suggested that *Ta. chingkankouensis* and *Ta. laiyangensis* are both *nomen dubium* because both of them have a serial of typical hadrosaurid characters, especially saurolophine characters, which distinguished from the non-hadrosaurid hadrosauroid, *Ta. sinensis*. Although some material of *Ta. chingkankouensis* could not be used for comparison due to the preservation problem, we still considered the diagnoses above are trustworthy by our anatomical

examinations and the original description of *Ta. chingkankouensis*. Our comparison among *Laiyangosaurus* (IVPP V 23402.15), *Ta. chingkankouensis* (IVPP V 724, a nearly complete sacrum and a partial right ilium) (Young, 1958) and *Ta. laiyangensis* (BMNH PH00181, a nearly complete sacrum associated with a partial right ilium) (Zhen, 1976; Zhang et al., 2019) shows that all of the ilia have a proportionately dorsoventrally low central plate of the ilium with the depth/length ratio <0.80 , which is a typical saurolophine character. Although the ilium (IVPP V 23402.15) has a symmetrical supraacetabular process and a well-defined ridge from the lateroventral margin of the supraacetabular process to the dorsal margin of the postacetabular process, which is different from asymmetrical supra-acetabular process and lack ridge between the supraacetabular process and the postacetabular process in BMNH PH00181, while the ilium of IVPP V 724 has the ridge but with asymmetrical supraacetabular process. Above differences of supraacetabular process would be due to the ilium IVPP V 23402.15 belonging to a juvenile of *Laiyangosaurus*. This situation was reported between the juvenile and adult specimens in *Edmontosaurus annectens* (Prieto-Márquez, 2014). Both IVPP V 23402.15 and IVPP V 724 display a brevis shelf and medial ridge at the base of the iliac postacetabular process, while the iliac postacetabular process missed in BMNH PH00181. Zhang et al. (2019) suggested that the ilium IVPP V 724 with a highly asymmetrical, U-shaped supraacetabular process with a well-defined caudoventral margin, would belong to *Tsintaosaurus*, and the relative warp analysis on the lateral outline of the supraacetabular process reveals a close resemblance of shape between BMNH PH00181 and *Secernosaurus*. Our anatomical comparison reveals that the ilia IVPP V 23402.15, IVPP V 724, and BMNH PH00181 share some striking features, and in the view of the ontogenetic changes of the supraacetabular process of ilium, and the collected location and stratum of *Laiyangosaurus* is neighbor with IVPP V 724 and BMNH PH00181, we suggest that IVPP V 724 and BMNH PH00181 represented as *Laiyangosaurus* material and that *Laiyangosaurus* shares some characters with *Secernosaurus*.

5 | CONCLUSION

This study provides postcranial characteristics to *Laiyangosaurus youngi* and supports the previous phylogenetic result of *L. youngi* lying in the Edmontosaurini clade. Three new postcranial autapomorphies can help distinguish *L. youngi* from other members of Edmontosaurini: poorly expanded deltopectoral crest of the humerus, a brevis shelf at the base of the postacetabular process of the ilium, and a well-

defined medioventral ridge on the medial side of the postacetabular process. The postcranial elements of *L. youngi* provide new evidence for comparing and discussing the taxonomic position and confirm its validity of hadrosauroids in the Laiyang Hadrosauroid Fauna.

AUTHOR CONTRIBUTIONS

Jialiang Zhang: Conceptualization; formal analysis; investigation; methodology; writing – original draft. **Xiaolin Wang:** Conceptualization; funding acquisition; investigation; methodology; resources; writing – review and editing. **Shunxing Jiang:** Conceptualization; formal analysis; funding acquisition; investigation; methodology; writing – review and editing. **Guobiao Li:** Conceptualization; funding acquisition; methodology; writing – review and editing.

ACKNOWLEDGMENTS

We thank Long Xiang, Hongjiao Zhou, Ruijie Wang, and Shiliang Cheng (IVPP) for preparing the specimens described here, Wei Gao (IVPP) for taking some of the photos that illustrate this article, Chuang Zhao for the reconstruction figure of *Laiyangosaurus*. We thank Qingjin Meng, Yuguang Zhang, and Di Liu (National Natural History Museum of China) for accessing the specimen. We are also indebted to Yan Li, Wei Gao, Long Xiang, Hongjiao Zhou, Ruijie Wang, Xing Cheng, Ning LI, Rui Qiu, He Chen, Xinjun Zhang, Rui Pan, Shiliang Cheng, and Huaquan Shou (IVPP) for assistance in the fieldwork. This study was supported by the Laiyang Cretaceous Fauna Research Program of the China University of Geosciences, Beijing (H02657), the National Natural Science Foundation of China (42288201 and 41172018), the Youth Innovation Promotion Association of Chinese Academy of Sciences (2019075), and the Laiyang Government Cooperation Dinosaur Project.

ORCID

Jialiang Zhang  <https://orcid.org/0009-0002-2082-2338>

REFERENCES

- Bolotsky, Y. L., & Godefroit, P. (2004). A new hadrosaurine dinosaur from the Late Cretaceous of Far Eastern Russia. *Journal of Vertebrate Paleontology*, 24(2), 351–365.
- Brett-Surman, M. K. (1979). Phylogeny and palaeobiogeography of hadrosaurian dinosaurs. *Nature*, 277, 560–562.
- Brett-Surman, M. K., & Wagner, J. R. (2006). Discussion of character analysis of the appendicular anatomy in Campanian and Mastrichtian north American hadrosauroids-variation and ontogeny. In K. Carpenter (Ed.), *Horns and Beaks: Ceratopsian and ornithomimid dinosaurs* (pp. 135–169). Indiana University Press.
- Brown, B. (1916). A new crested trachodont dinosaur *Prosaurolophus maximus*. *Bulletin of the American Museum of Natural History*, 35, 701–708.

- Buffetaut, E., & Tong, H. Y. (1993). *Tsintaosaurus spinorhinus* Young and *Tanius sinensis* Wiman: A preliminary comparative study of two hadrosaurs (Dinosauria) from the upper cretaceous of China. *Comptes Rendus de l'Académie des sciences. Série 2, Mécanique, physique, Chimie, sciences de l'univers, Sciences de la Terre*, 317(9), 1255–1261.
- Buffetaut, E., & Tong, H. Y. (1995). The late cretaceous dinosaurs of Shandong, China: Old finds and new interpretations. In A. L. Sun & Y. Q. Wang (Eds.), *Sixth symposium on Mesozoic terrestrial ecosystems and biota* (pp. 139–142). China Ocean Press.
- Cuthbertson, R. S. (2006). A redescription of the holotype of *Brachylophosaurus canadensis* (Dinosauria: Hadrosauridae), with a discussion of chewing in hadrosaurs. PhD dissertation. Carleton University, Ottawa, Ontario, 128 p.
- Gilmore, C. W. (1933). On the dinosaurian fauna of the Iren Dabasu formation. *Bulletin of the American Museum of Natural History*, 67, 23–78.
- Godefroit, P., Bolotsky, Y. L., & Lauters, P. (2012). A new saurolophine dinosaur from the latest cretaceous of far eastern Russia. *PLoS One*, 7(5), e36849.
- Godefroit, P., Bolotsky, Y. L., & van Itterbeeck, J. (2004). The lambeosaurine dinosaur *Amurosaurus riabinini*, from the Maastrichtian of far eastern Russia. *Acta Palaeontologica Polonica*, 49(4), 585–618.
- Goloboff, P. A., Farris, J. S., & Nixon, K. (2008). TNT, a free program for phylogenetic analysis. *Cladistics*, 24(5), 774–786.
- Horner, J. R., Weishampel, D. B., & Forster, C. A. (2004). Hadrosauridae. In D. B. Weishampel, P. Dodson, & H. Osmólska (Eds.), *The dinosauria* (2nd ed., pp. 438–463). University of California Press.
- Hu, C. Z. (1973). A new hadrosaur from the cretaceous of Zhucheng, Shantung. *Acta Geologica Sinica*, 2, 179–202.
- Hu, C. Z., Cheng, Z. W., Pang, Q. Q., & Fang, X. S. (2001). *Shantungosaurus giganteus* (p. 116). Geological Publishing House.
- Juárez Valieri, R. D., Haro, J. A., Fiorelli, L. E., & Calvo, J. O. (2010). A new hadrosauroid (Dinosauria: Ornithopoda) from the Allen Formation (late cretaceous) of Patagonia, Argentina. *Revista del Museo Argentino de Ciencias Naturales*, 12(2), 217–231.
- Lambe, L. M. (1914). *On Gryposaurus notabilis, a new genus and species of trachodont dinosaur from the Belly River formation of Alberta, with description of the skull of Chasmosaurus belli* (Vol. 27, pp. 145–155). Ott Nat.
- Lambe, L. M. (1917). A new genus and species of crestless hadrosaur from the Edmonton Formation of Alberta. *The Ottawa Naturalist*, 31(7), 65–73.
- Lund, E. K., & Gates, T. A. (2006). A historical and biogeographical examination of hadrosaurian dinosaurs. *Bulletin—New Mexico Museum of Natural History and Science*, 35, 263–276.
- Marsh, O. C. (1892). Notice of new reptiles from the Laramie formation. *American Journal of Science*, 3(257), 449–453.
- Maryanska, T., & Osmólska, H. (1984). Postcranial anatomy of *Saurolophus angustirostris* with comments on other hadrosaurs. *Palaeontologia Polonica*, 46, 119–141.
- Mateus, O., Polcyn, M. J., Jacobs, L. L., Araújo, R., Schulp, A. S., Marinherio, J., Pereira, B., & Vineyard, D. (2012). Cretaceous amniotes from Angola: Dinosaurs, pterosaurs, mosasaurs, plesiosaurs, and turtles. In *Actas de V Jornadas Internacionales sobre Paleontología de Dinosaurios y su Entorno, Salas de los Infantes, Burgos* (pp. 71–105). Colectivo Arqueológico y Paleontológico de Salas.
- Mori, H., Druckenmiller, P. S., & Erickson, G. M. (2015). A new Arctic hadrosaurid from the Prince Creek formation (lower Maastrichtian) of northern Alaska. *Acta Palaeontologica Polonica*, 61(1), 15–32.
- Prieto-Márquez, A. (2007). Postcranial osteology of the hadrosaurid dinosaur *Brachylophosaurus canadensis* from the late cretaceous of Montana. In *Horns and beaks. Ceratopsian and ornithomimid dinosaurs* (pp. 91–115). Indiana University Press.
- Prieto-Márquez, A. (2008). Phylogeny and historical biogeography of hadrosaurid dinosaurs. PhD dissertation, Florida State University, Tallahassee, Florida, 936 p.
- Prieto-Márquez, A. (2010a). Global historical biogeography of hadrosaurid dinosaurs. *Zoological Journal of the Linnean Society*, 159, 503–525.
- Prieto-Márquez, A. (2010b). Global phylogeny of Hadrosauridae (Dinosauria: Ornithopoda) using parsimony and Bayesian methods. *Zoological Journal of the Linnean Society*, 159, 435–502.
- Prieto-Márquez, A. (2011). The skull and appendicular skeleton of *Gryposaurus latidens*, a saurolophine hadrosaurid (Dinosauria: Ornithopoda) from the early Campanian (cretaceous) of Montana, USA. *Canadian Journal of Earth Sciences*, 49, 510–532.
- Prieto-Márquez, A. (2014). A juvenile *Edmontosaurus* from the late Maastrichtian (cretaceous) of North America: Implications for ontogeny and phylogenetic inference in saurolophine dinosaurs. *Cretaceous Research*, 50, 282–303.
- Prieto-Márquez, A., Erickson, G. M., & Ebersole, J. A. (2016). A primitive hadrosaurid from southeastern north America and the origin and early evolution of 'duck-billed' dinosaurs. *Journal of Vertebrate Paleontology*, 36(2), e1054495.
- Tan, X. C. (1923). New research on the Mesozoic and early tertiary geology in shantung. *Bulletin of the Geological Survey of China*, 5(2), 95–135.
- Wang, Q., Wang, X. L., Zhao, Z. K., Zhang, J. L., & Jiang, S. X. (2013). New turtle egg fossil from the upper cretaceous of the Laiyang Basin, Shandong Province, China. *Anais da Academia Brasileira de Ciências*, 85(1), 103–111.
- Wang, R. F., You, H. L., Xu, S. C., Wang, S. Z., Yi, J., Xie, L. J., Jia, L., & Li, Y. X. (2013). A new hadrosauroid dinosaur from the early late cretaceous of Shanxi Province, China. *PLoS One*, 8(10), e77058.
- Wang, X. L., Wang, Q., Jiang, S. X., Chen, X., Zhang, J. L., Zhao, Z. K., & Jiang, Y. G. (2012). Dinosaur egg faunas of the upper cretaceous terrestrial red beds of China and their stratigraphical significance. *Journal of Stratigraphy*, 36(2), 400–416.
- Wang, X. L., Wang, Q., Wang, J. H., Zhang, J. L., Cheng, X., Jiang, S. X., & Pan, R. (2010). An overview on the cretaceous dinosaurs and their eggs from Laiyang, Shandong Province, China. In W. Dong (Ed.), *Proceedings of the twelfth annual meeting of the Chinese Society of vertebrate paleontology* (pp. 293–316). China Ocean Press.
- Wiman, C. (1929). Die Kreide-Dinosaurier aus Shantung. *Palaeontologica Sinica Series C*, 6(1), 1–67.
- Xing, H., Wang, D. Y., Han, F. L., Sullivan, C., Ma, Q. Y., He, Y. M., Hone, D. W. E., Yan, R. H., Du, F. M., & Xu, X. (2014). A new basal hadrosauroid dinosaur (Dinosauria: Ornithopoda) with transitional features from the late cretaceous of Henan Province, China. *PLoS One*, 9(6), e98821.
- Xing, H., Zhao, X. J., Wang, K. B., Li, D. J., Chen, S. Q., Mallon, J. C., Zhang, Y. X., & Xing, X. (2014). Comparative

osteology and phylogenetic relationship of Edmontosaurus and Shantungosaurus (Dinosauria: Hadrosauridae) from the upper cretaceous of North America and East Asia. *Acta Geologica Sinica-English*, 88(6), 1623–1652.

Yan, J., & Chen, J. F. (2005). Clinopyroxene megacrysts in the late Mesozoic basalts from Da, Jiaozhou. *Journal of Anhui University of Technology (Natural Science)*, 25(3), 9–13.

You, H. L., Luo, Z. X., Shubin, N. H., Witmer, L. M., Tang, Z. L., & Tang, F. (2003). The earliest-known duck-billed dinosaur from deposits of late early cretaceous age in Northwest China and hadrosaur evolution. *Cretaceous Research*, 24, 347–355.

Young, C. C. (1958). *The dinosaurian remains of Laiyang, Shantung. Palaeontologia sinica* New Series C16 (pp. 1–138). Science Press.

Zhang, J. L., Wang, X. L., Wang, Q., Jiang, S. X., Cheng, X., Li, N., & Qiu, R. (2017). A new saurolophine hadrosaurid (Dinosauria: Ornithopoda) from the upper cretaceous, Shandong, China. *Annals of the Brazilian Academy of Sciences. Anais Da Academia Brasileira De Ciências*, 91, e20160920.

Zhang, Y. G., Wang, K. B., Chen, S. Q., Liu, D., & Xing, H. (2019). Osteological re-assessment and taxonomic revision of “*Tanius laiyangensis*” (Ornithischia: Hadrosauoidea) from the upper cretaceous of Shandong, China. *The Anatomical Record*, 303(4), 790–800.

Zhen, S. N. (1976). A new species of hadrosaur from Shandong. *Vertebrata PalAsiatica*, 14(3), 166–168.

How to cite this article: Zhang, J., Wang, X., Jiang, S., & Li, G. (2023). The postcranial anatomy of the saurolophine hadrosaurid *Laiyangosaurus youngi* from the upper cretaceous of Laiyang, Shandong, China. *The Anatomical Record*, 1–17. <https://doi.org/10.1002/ar.25291>

APPENDIX A

Character state scores of *L. youngi* for the 273 characters presented by Prieto-Márquez et al. (2016). The scores for all the other taxa included in the analysis are as in Prieto-Márquez et al. (2016).

[0 1]??0????01[1 2]102?????????1[0 1]0110011021110
 011????31?????????0?10-?00??-??-?11?[0 1]220211112321-
 00??1000110?110?????????????????2?????????????????
 ??????????1?1?-??-01112-00-----?????????0??11?????1?11?
 11-11200?1?????????1?????2?1211301111?????110111?0212
 21?0---111???????